Stress-Drop Variability of Shallow Earthquakes Extracted from a Global Database of Source Time Functions

by Françoise Courboulex, Martin Vallée, Matthieu Causse, and Agnès Chounet

ABSTRACT

We use the new global database of source time functions (STFs) and focal mechanisms proposed by Vallée (2013) using the automatic SCARDEC method (Vallée *et al.*, 2011) to constrain earthquake rupture duration and variability. This database has the advantage of being very consistent since all the events with moment magnitudes $M_w > 5.8$ that have occurred during the last 20 years were reanalyzed with the same method and the same station configuration. We analyze 1754 shallow earthquakes (depth < 35 km) and use high-quality criteria for the STFs, which result in the selection of 660 events. Among these, 313 occurred on the subduction interface (SUB events) and 347 outside (NOT-SUB events). We obtain that for a given magnitude, STF duration is log normally distributed and that STFs are longer for SUB than NOT-SUB events. We then estimate the stress drop using a proxy for the rupture process duration obtained from the measurement of the maximum amplitude of the STF. The resulting stress drop is independent of magnitude and is about 2.5 times smaller for the subduction events compared with the other events. Assuming a constant rupture velocity and source model, the resulting standard deviation of the stress drop is 1.13 for the total dataset (natural log), and about 1 for separate datasets. These values are significantly lower than the ones generally obtained from corner-frequency analyses with global databases (~1.5 for Allmann and Shearer, 2009) and are closer to the values inferred from strong-motion measurements (~0.5 as reported by Cotton *et al.*, 2013). This indicates that the epistemic variability is reduced by the use of STF properties, which allows us to better approach the natural variability of the source process, related to stress-drop variability and/or variation in the rupture velocity.

INTRODUCTION

Numerous parameters are required to estimate in advance the ground motion caused by an earthquake. The first-order parameters are the magnitude M of the earthquake and its distance to the observation point. The second-order parameters are linked both to attenuation and sometimes amplification at the regional and local scale (anelastic attenuation and site effect) and to the source process itself. The source parameter generally recognized as the most important for the control of high frequencies is the stress-drop $\Delta\sigma$ (Hanks and McGuire, 1981). This parameter is, in fact, directly or indirectly an input of most of the ground-motion simulation methods (see Douglas and Aochi, 2008). Determination of stress drop is thus a major concern for the prediction of high-frequency ground motions (e.g., peak ground acceleration [PGA] and peak ground velocity levels). It is first important to mention that the term stress drop is not used unequivocally. As pointed out by Atkinson and Beresnev (1997), it can reflect various concepts that are not always associated with its true physical meaning, which is simply the difference between the stress level before and after an earthquake. We introduce hereafter the commonly used definitions of stress drop.

The original definition of stress drop is referred to as static stress drop and was introduced as a measure of the static deformation induced by an earthquake. As such, it is directly related to the strain drop, that is the ratio of seismic slip over the dimension of the rupture (Kanamori and Boschi, 1983; Vallée, 2013). The stress drop averaged over the fault plane can be simply expressed by

$$\Delta\sigma \approx \mu\bar{D}/L, \tag{1}$$

in which μ, $\bar{D}$, and L are the earth rigidity, the average slip on the fault, and a characteristic rupture dimension. For a constant seismic moment, the stress drop is thus higher when the rupture surface is small and the average displacement is high. In a bidimensional source model, the stress drop is equal to:

$$\Delta\sigma = cM_0/L^3, \tag{2}$$

in which M_0 is the seismic moment and c is a factor depending on the rupture type (Kanamori and Rivera, 2004). The rupture dimension is thus a key parameter to determine $\Delta\sigma$, but its value is inaccessible to direct observation. For large earthquakes ($M \gtrsim 7$), the rupture dimension is often retrieved by the inversion of several datasets: teleseismic and/or local seismograms and/or geodetic measurements (see the database of finite-source rupture models compiled by Mai and Thingbaijam, 2014). The rupture dimension can also be deduced from the distribution of early aftershocks. For superficial events that break the surface, direct rupture length measurements can also be used (e.g., Wells and Coppersmith, 1994; Manighetti *et al.*, 2007; Shaw, 2013). The smaller (and more numerous) earthquakes, however, are not systematically studied with such detailed analyses. It is the case only for some specific earthquakes in well-instrumented areas that had a strong impact on populated regions, for example, the recent 2015 Napa Valley earthquake or the 2009 L'Aquila event (e.g., Tinti *et al.*, 2014; Dreger *et al.*, 2015), among many others. Thus, even if static stress drop is directly related to the stress release on the fault, it has limited practical utility due to the difficulty in measuring slip and fault dimensions.

An alternative way to assess stress drop is to use seismological parameters that are easier to measure. For instance, the duration of the source time function (STF), representative of the total duration of the source process T, can be inferred from distant seismograms. Introducing the rupture velocity V_r, equation (2) becomes:

$$\Delta\sigma = cM_0/(V_rT)^3. \quad (3)$$

Thus, for a given seismic moment, a similar value of the stress drop can be obtained for a short STF duration and a high rupture velocity, or for a long STF duration and a low rupture velocity. It is well known from source studies that V_r values usually vary in the range (0.6–0.9 V_S) (e.g., Heaton, 1990) and sometimes exceed, for a portion of the rupture, the shear-wave velocity (e.g., Bouchon *et al.*, 2001; Dunham and Archuleta, 2004; Walker and Shearer, 2009; Vallée and Dunham, 2012). Nevertheless, because V_r is difficult to obtain and is apparently not linked with M_0, most of the studies simply assume that V_r is constant and then put their efforts into determining T, which is much more variable and correlated with M_0.

Practically, most of the studies using seismograms to determine stress drop are based on the corner-frequency f_c determination. f_c is generally defined on the Fourier spectrum in displacement (Thatcher and Hanks, 1973; Allmann and Shearer, 2009) as the intersection between a flat low-frequency level and an f^{-2} slope that describes the fall off of the high frequencies in the ω^{-2} model (Brune, 1971). The relationship often used to link f_c and the stress drop assumes a circular crack model:

$$\Delta\sigma = \frac{7}{16} M_0 f_c^3/(kV_s)^3, \quad (4)$$

in which k depends on the assumptions of the rupture model and on the type of wave. For instance, Brune (1971) used $k = 0.37$ for S waves, whereas $k = 0.21$ for Madariaga (1976) and $k = 0.26$ for Kaneko and Shearer (2014). Tests of k values for different source models can be found in Dong and Papageorgiou (2003). Note that stress drop is proportional to the cube of f_c in equation (4) and the cube of T in equation (3). Its determination is then highly sensitive to these values. Determining the absolute value of an earthquake stress drop is then both sensitive to the selected parameters and to the measurements made on the data. In this article, we do not focus on the absolute values of stress drop, but rather on its relative values and variability.

A recent article by Cotton *et al.* (2013) examines the links between the variability of the seismic stress drop, hereafter called $\mathrm{sigma}_{\ln}(\Delta\sigma)$, determined on seismologic data, and the variability of the PGA, $\mathrm{sigma}_{\ln}(\mathrm{PGA})$, reported in ground-motion prediction equations (GMPEs) for between-event variability (Al-Atik *et al.*, 2010). Based on the theory of random vibrations (Hanks and McGuire, 1981), and assuming a constant rupture velocity, the relationship should be: $\mathrm{sigma}_{\ln}(\Delta\sigma) = 1.25\ \mathrm{sigma}_{\ln}(\mathrm{PGA})$. Cotton *et al.* (2013) then compare the stress-drop variability obtained by different authors on global seismological databases and the variability obtained from GMPEs. They note that the variability obtained from seismological data is much larger than that deduced from GMPEs. They attribute this difference to a possible overestimation of $\mathrm{sigma}_{\ln}(\Delta\sigma)$ due to the difficulty in measuring the f_c value.

We then propose to remeasure this variability from a database of STFs recently made available that analyzes all the earthquakes with $M_w > 5.8$ of the last 20 years. Unlike global databases that typically used f_c to calculate the stress-drop variations (Allmann and Shearer, 2009, being the most recent and complete), the SCARDEC database directly produces STFs that avoids the need of a corner-frequency estimation. In this article, we analyze the stress-drop variations directly estimated from these STFs and make subsets of earthquakes to examine their σ values.

STF DURATION DETERMINATION FROM THE SCARDEC DATABASE

A recently developed method, called SCARDEC (Vallée *et al.*, 2011), provides simultaneous access to the focal mechanism, seismic moment, depth, and STFs of most earthquakes with moment magnitude $M_w > 5.8$. As SCARDEC is fully automated, the STFs can be obtained for an unprecedented number of earthquakes (2892 events analyzed from 1992 to 2014). The STF determination is obtained by deconvolution of teleseismic waveforms by a Green's function computed in the global IASP91 model (Kennett and Engdahl, 1991). The STF obtained must be causal and positive, and its integral (which corresponds to the seismic moment) must be constant at each station.

Because our aim is to reduce the epistemic uncertainty and to have better access to the natural variability of the source process, we work on a restricted database. We first exclude the strike-slip events whose STF determination is generally more complex and often poorly constrained by P-wave analysis, and also all the events which do not provide a fully consistent STF determination (based on the measurement of the teleseismic interstation STF coherence). This can occur because of focal

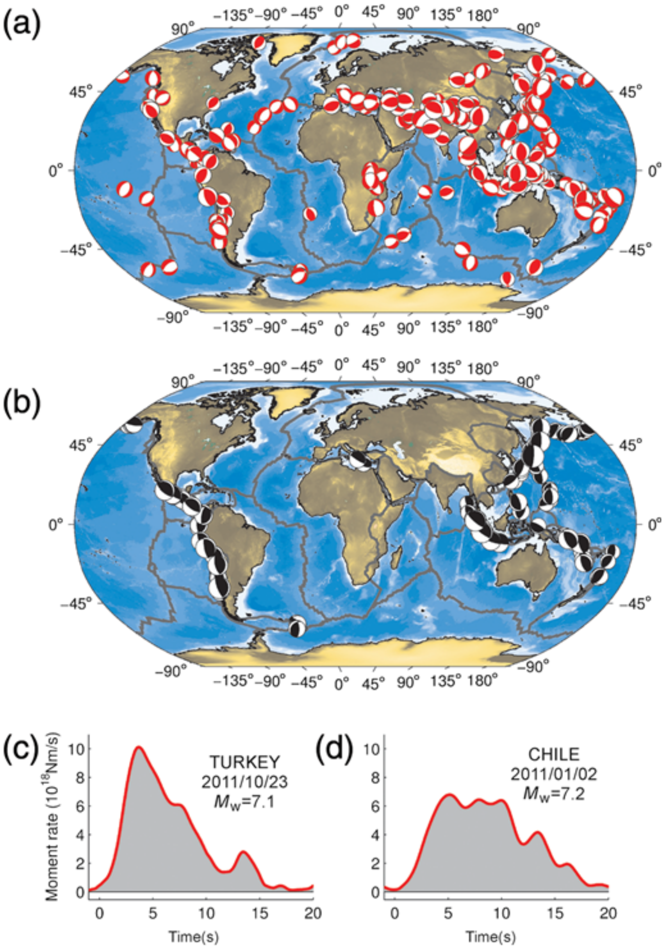

▲ **Figure 1.** Source time function (STF) database of shallow earthquakes (depth < 35 km) used in this study, built using the SCARDEC method (Vallée *et al.*, 2011). (a) Focal mechanism and geographical distribution of the 347 nonsubduction selected events. (b) Focal mechanism and geographical distribution of the 313 subduction selected events. (c) Example of STF for a nonsubduction earthquake (Van earthquake). (d) Example of STF for a subduction earthquake. Note that even if the Van earthquake has a slightly smaller magnitude, the STF duration is shorter and its peak F_m is larger, which illustrates the behavior statistically observed in the database. The color version of this figure is available only in the electronic edition.

mechanism complexities, large rupture depth extent, and strong directivity effects (e.g., Ben-Menahem, 1962; Ammon *et al.*, 2006, Vallée, 2007; Courboulex *et al.*, 2013). Finally, we restrict our analysis to shallow events (depth < 35 km), whose influence on ground motions is stronger than deeper ones. In the database of 1754 shallow events, 660 are then selected based on the previous criteria. Among them, 313 occurred on the subduction interface and 347 outside (Fig. 1a and 1b).

The total duration T of the STF obtained is not simple to determine. Indeed, the practical determination of T may suffer from subjective criteria to determine when the STFs actually begin and end. Moreover, the relation between the total duration and the source process characteristics (stress drop in particular) is biased when the STF displays two or more slip patches separated in time. Another approach is to measure the peak value of the STF (maximum moment rate) F_m, and to compute a characteristic duration from F_m and M_0 (using, for example, a triangular shape for the STF). In this case, the presence of a late complexity of the STF only has a minor effect on the characteristic duration. This method has been preferred by Vallée (2013) for a more robust and consistent determination of the duration.

In our study, we test the two approaches. We first measure a STF-duration-based T as the duration of the STF between the first amplitude above $0.1F_m$ with increasing trend, and the last amplitude above $0.1F_m$ with decreasing trend. We then measure an F_m-based T as the width of the isosceles triangular-shaped STF with same maximum F_m and area M_0: $T = 2M_0/F_m$. We find overall similar results for both approaches, but the variability of T (standard deviation of $\ln[T]$), hereafter referred as $\text{sigma}_{\ln}(T)$ is always reduced when using F_m instead of the STF duration. The mean duration obtained being almost the same, we chose to determine T from F_m for the following analysis. We found that $\text{sigma}_{\ln}(T)$ has values between 0.3 and 0.4 (natural log) without any clear dependence on the magnitude.

STF DURATION IN DIFFERENT CONTEXTS

We separate the SCARDEC dataset into two main subsets: subduction events, that is, thrust events occurring on the subduction interface (SUB), and all the other event types (NOT-SUB). It is clear from Figure 2a that the STF duration T is longer for subduction events than for the others (an illustration of this behavior is shown in Fig. 1c and 1d for two earthquakes belonging to each of the contexts). This has been pointed out by Chounet and Vallée (2014) with the SCARDEC database and already observed in other global databases (Kanamori and Anderson, 1975; Bilek and Lay, 1999; Houston, 2001; Allmann and Shearer, 2009). Active and well-developed subduction plate boundaries can lead to smoother ruptures; also, the hydration of the contact can weaken the frictional properties. Those two features may induce lower rupture velocity and/or lower stress-drop earthquakes. Simple regressions can be obtained for both regions (Fig. 2a).

Our next goal is to estimate the duration distribution for earthquakes of a given magnitude M_w. To have a sufficiently large amount of data, we compute this distribution using earthquakes with moment magnitude of $M_w \pm 0.3$. Variations of T due to variation of magnitude inside this range are scaled to be comparable. The STF duration $T(s)$ roughly follows a lognormal distribution (see Fig. 2b, bottom, an example for M_w 6.4) with $\text{sigma}_{\ln}(T) = 0.37$ for the whole dataset, 0.32 for subduction events and 0.34 for the others.

IMPLICATION FOR STRESS DROP

If, like many authors, we use equation (4) for a circular crack to determine stress drop, we have to determine k and V_S and we

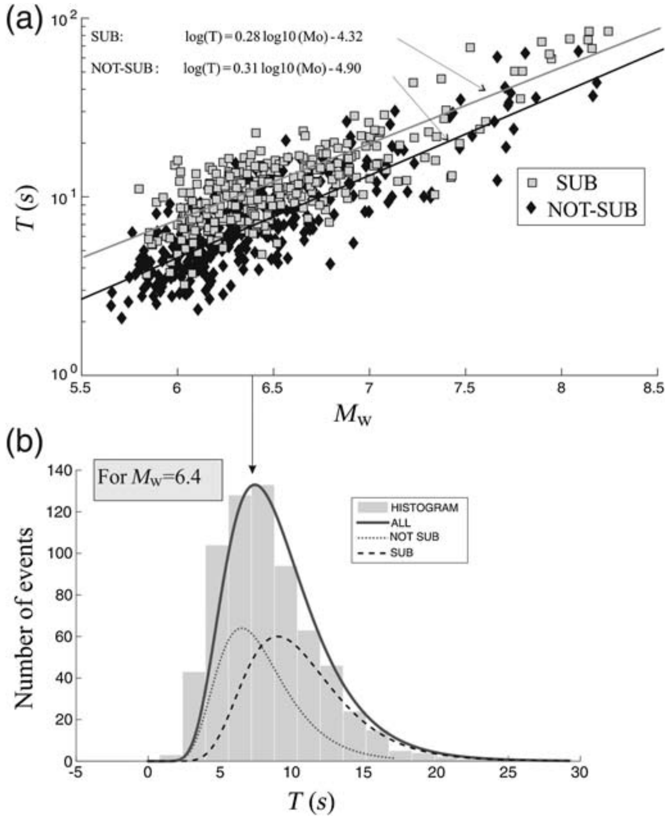

▲ **Figure 2.** (a) STF duration (obtained from F_m measurements) versus magnitude (M_w) for earthquakes that occur on the subduction interface (SUB) and away from it (NOT-SUB). Linear regressions are represented for both subsets. (b) Histogram of $T(s)$ values for events with M_w 6.4 $\pm$ 0.3 (a correction is applied to account for the differences of magnitude). Lines correspond to the lognormal function that best fits the total distribution (bold line), the NOT-SUB subset (gray dotted line) and the SUB subset (black dotted line).

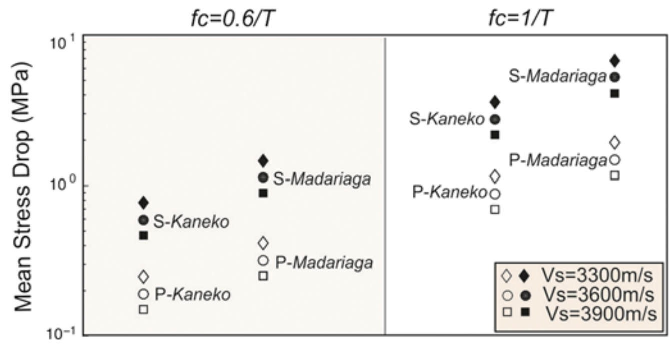

▲ **Figure 3.** Variation of the mean stress-drop values obtained from the SCARDEC database using two relationships between the total duration T and f_c, three values of V_S from 3300 to 3900 m/s and four values of k: P Madariaga corresponds to $k = 0.32$ for P waves and S Madariaga to $k = 0.21$ for S waves (Madariaga, 1976). P Kaneko corresponds to $k = 0.38$ and S Kaneko to $k = 0.26$ (Kaneko and Shearer, 2014) for P and S waves. The color version of this figure is available only in the electronic edition.

also have to convert the values of T obtained from the SCARDEC database into f_c values. This T–f_c relationship is dependent on the source model (see the appendix of Godano *et al.*, 2015). In some classes of STF models (Brune's STF, isosceles triangle), the relation between f_c and the inverse of the half-pulse duration is very close to 0.3 (Madariaga, 1976; Kaneko and Shearer, 2015; Madariaga, personal comm.). For example, it can be simply shown from the Fourier transform that the coefficient for the isosceles triangle is $1/\pi$. These models would therefore lead to $fc \sim 0.6/T$. However, if referring to the Haskell model, the relation is closer to $f_c = 1/T$.

To quantify the influence of the input parameters of equation (4) on the mean stress drop, we test V_S values from 3300 to 3900 m/s, k values for Madariaga (1976) and Kaneko and Shearer (2014) models for P and S waves and two relationships between f_c and T ($f_c = 0.6/T$ and $f_c = 1/T$). Note that it is assumed that the rupture velocity V_r is linked with the shear-wave velocity by a constant relationship $V_r = 0.9V_S$. As expected, we obtain a very large variation of the mean values, mainly influenced by the choice of k and the relationship between T and f_c (Fig. 3). For this reason, the absolute stress-drop value has to be analyzed with caution.

To obtain a general view of the stress-drop variability with the SCARDEC database for a given model, we select fixed values for equation 4: $k = 0.32$ (for P waves and Madariaga model), $V_S = 3900$ m/s (value chosen by Allmann and Shearer, 2009) and the relation $f_c = 0.6/T$ justified above. The stress drop obtained (Fig. 4a) does not depend on magnitude (mean values are almost constant), in accordance with the self-similarity assumption widely accepted for earthquakes with magnitude larger than 5, and already shown by Vallée (2013) for SCARDEC database.

If we now compare the mean stress-drop values obtained for the selected dataset, SUB and NOT-SUB datasets, we obtain a stress-drop value about 2.5 times smaller for the subduction events compared to the other events (Fig. 5a).

The variability of the stress drop $\text{sigma}_{\ln}(\Delta\sigma)$ is almost constant with magnitude, with a slight increase for larger values (Fig. 5b). This may simply arise from the smaller number of events with larger magnitudes, for which the influence of one single event may then be more important. The value of $\text{sigma}_{\ln}(\Delta\sigma)$ is about 1.13 for the whole selected dataset. It is slightly smaller for NOT-SUB events (1.03) and even smaller for SUB events (0.98) (Fig. 5b).

DISCUSSION AND CONCLUSION

Stress-drop variability is the subject of many studies that aim to better understand and constrain both source processes on faults and ground-motion predictions. Many different datasets have been used by several authors to try to constrain this value. Using surface-slip observations, Manighetti *et al.* (2007) found $\text{sigma}_{\ln}(\Delta\sigma) = 0.9$ from 250 continental earthquakes and Shaw

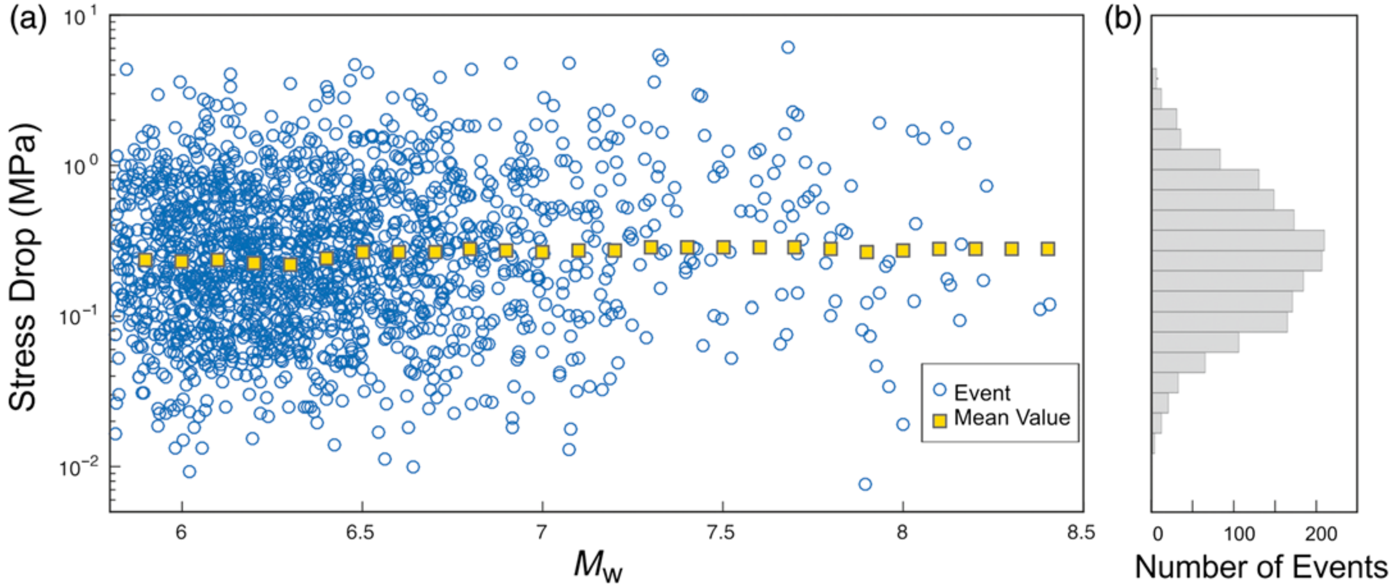

▲ **Figure 4.** (a) Stress-drop values (MPa) obtained from the SCARDEC catalog of STF for shallow earthquakes (depth < 35 km) using equation (4) for $k = 0.32$ (value for P waves in the Madariaga, 1976, model), $V_S = 3900$ m/s and $f_c = 0.6/T$. Mean values are computed for bins of $M_w \pm 0.1$. (b) Distribution of $\log_{10}(\Delta\sigma)$. The color version of this figure is available only in the electronic edition.

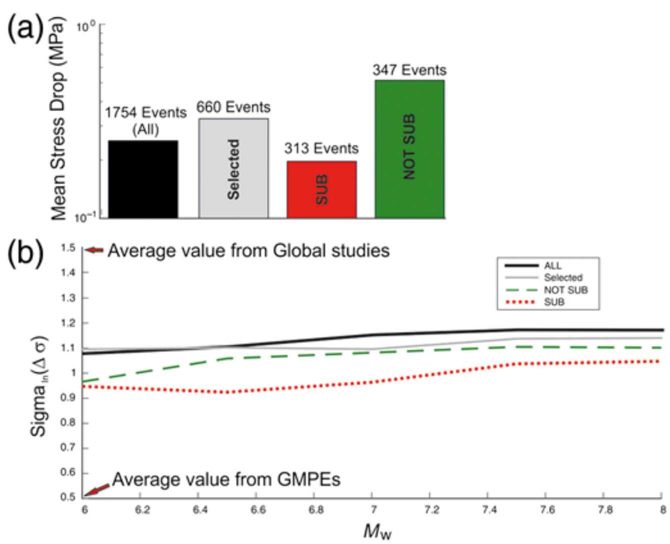

▲ **Figure 5.** (a) Mean stress-drop values obtained for the whole database, the selected database, SUB and NOT-SUB datasets. Stress-drop values are mean values computed using equation (4), with $V_S = 3900$ m/s, $k = 0.32$ and $f_c = 0.6$/T. (b) sigma$_{\ln}(\Delta\sigma)$ with magnitude for all events (for ± 0.1 bins), the selected events, and the SUB and NOT-SUB subsets. The values obtained by Cotton *et al.* (2013) for source studies on global databases and derived from ground-motion prediction equations (GMPEs) are indicated. The color version of this figure is available only in the electronic edition.

(2013) found 0.7 from 37 strike-slip events. Similar values were obtained by Mai and Beroza (2000) (sigma$_{\ln}(\Delta\sigma) = 0.8$), using rupture surface and average slip derived from 31 slip inversion models of 18 earthquakes ($5.5 < \mathrm{M} < 8$), and by Causse *et al.* (2014) (sigma$_{\ln}(\Delta\sigma) = 0.7$) from finite-rupture models of 21 crustal events.

Using local or regional seismological data, Cotton *et al.* (2013) reported values from 0.57 (earthquakes in Greece, Margaris and Hatzidimitriou, 2002) to 1.83 (earthquakes in Switzerland, Edwards and Fäh, 2013), whereas Baltay *et al.* (2013) found a value of 0.9 for earthquakes in Japan. Nevertheless, our study is based on a global database, including hundreds of events with $M > 5.8$ recorded from 1992 to 2014. In this respect, the largest and most recent worldwide database has been built by Allmann and Shearer (2009). As reported by Cotton *et al.* (2013), Allmann and Shearer (2009) found sigma$_{\ln}(\Delta\sigma) = 1.67$ for interplate events and sigma$_{\ln}(\Delta\sigma) = 1.46$ for intraplate ones. For the same range of magnitudes, we obtained much lower values (around 1), which indicate that the use of the SCARDEC database significantly reduces epistemic variability. One of the reasons is likely related to the use of F_m, which is expected to be more meaningful than f_c-derived measurements, in particular when the source is complex: even in the case of an STF with several peaks, F_m can always be nonequivocally determined (while the concept of a single corner frequency becomes unclear), and the values derived from this peak moment rate will at least approximate the behavior of the dominant patch of the rupture.

To check the effects of the initial data selection procedure (removal of strike-slip earthquakes and events without a fully consistent determination of the STF), we also computed the sigma value considering all of the 1750 events with depths shallower than 35 km. We found a variability of the STF duration sigma$_{\ln}(\Delta T)$ equal to 0.38. The resulting sigma$_{\ln}(\Delta\sigma)$ equal to 1.14 is then only marginally larger than for the database of selected events (see the ALL dataset represented by a bold line in Fig. 5b). We can then suppose that a large part of the epistemic variability has been removed and that we are closer to the natural variability of the source process.

Nevertheless, the question raised by Cotton *et al.* (2013) remains open. Why is the variability obtained (around 1) still two times larger than the one derived from PGA between-event variability observed in ground-motion databases (e.g., Al-Atik *et al.*, 2010), which is generally around 0.5 (Cotton *et al.*, 2013). This result is surprising and counterintuitive. One would expect that the details of the high-frequency rupture process and the natural heterogeneity of the distribution of stress on the fault (e.g., Noda *et al.*, 2013) affect more the observed PGA than the full duration of the STF. The source duration, which is a global source property, should intuitively vary less than the corresponding PGA.

The large values of the stress-drop variability obtained from global seismological databases can be partially explained by the fact that the variability of the STF duration (or f_c) is always converted into stress drop using a single source model and fixed input parameters. It is probable that if the ad hoc parameters were specifically chosen for each earthquake, the stress-drop variability would be lower. It is also clear that the rupture velocity plays a major role in the variability of the corner frequency (Kaneko and Shearer, 2015) and of the STF duration (e.g., Kanamori and Rivera, 2004), and that a possible correlation or anticorrelation (as proposed by Causse and Song, 2015) between stress drop and rupture velocity would modify the stress-drop variability. The resolution of this problem must wait for more reliable determination of V_r and $\Delta\sigma$.

Finally, we cannot exclude that the low values of the stress-drop variability deduced from the PGA variability (Cotton *et al.*, 2013) arise from an underestimation of the observed between-event variability of PGA. In addition, the simple relationship used to relate PGA and static stress drop may be more complex in real cases.

DATA AND RESOURCES

Source time functions (STFs) can be obtained from SCARDEC database at http://scardec.projects.sismo.ipgp.fr (last accessed April 2016).

ACKNOWLEDGMENTS

We thank Annemarie Baltay, Adrian Oth, and Zhigang Peng for their constructive remarks that helped us to improve the article. This study has benefited from the comments of Raul Madariaga. It has been partially funded by Institut National de Sciences de l'Univers (CNRS) through CT3 project.

REFERENCES

Al-Atik, L., N. Abrahamson, J. J. Bommer, F. Scherbaum, F. Cotton, and N. Kuehn (2010). The variability of ground-motion prediction models and its components, *Seismol. Res. Lett.* **81,** 794–801.

Allmann, B. P., and P. M. Shearer (2009). Global variations of stress drop for moderate to large earthquakes, *J. Geophys. Res.* **114,** no. B01, 310, doi: 10.1029/2008JB005821.

Ammon, C. J., A. A. Velasco, and T. Lay (2006). Rapid estimation of first-order rupture characteristics for large earthquakes using surface waves: 2004 Sumatra-Andaman earthquake, *Geophys. Res. Lett.* **33,** no. 14, L14314, doi: 10.1029/2006GL026303.

Atkinson, G., and I. Beresnev (1997). Don't call it stress drop, *Seismol. Res. Lett.* **68,** 1–4.

Baltay, A. S., T. C. Hanks, and G. C. Beroza (2013). Stable stress-drop measurements and their variability: Implications for ground-motion prediction, *Bull. Seismol. Soc. Am.* **103,** no. 1, 211–222.

Ben-Menahem, A. (1962). Radiation of seismic body waves from a finite moving source in the earth, *J. Geophys. Res.* **67,** no. 1, 345–350.

Bilek, S. L., and T. Lay (1999). Rigidity variations with depth along interplate megathrust faults in subduction zones, *Nature* **400,** 6743, 443–446.

Bouchon, M., M. Bouin, H. Karabulut, M. N. Toksöz, M. Dietrich, and A. J. Rosakis (2001). How fast is rupture during an earthquake? New insights from the 1999 Turkey earthquakes, *Geophys. Res. Lett.* **28,** no. 14, 2723–2726.

Brune, J. N. (1971). Seismic sources, fault plane studies and tectonics, *Eos Trans. AGU* **52,** no. 5, IUGG 178–IUGG 187.

Causse, M., and S. G. Song (2015). Are stress drop and rupture velocity of earthquakes independent? Insight from observed ground motion variability, *Geophys. Res. Lett.* **42,** no. 18, 7383–7389.

Causse, M., L. A. Dalguer, and P. M. Mai (2014). Variability of dynamic source parameters inferred from kinematic models of past earthquakes, *Geophys. J. Int.* **196,** 1754–1769, doi: 10.1093/gji/ggt478.

Chounet, A., and M. Vallée (2014). Systematic characterization of radiated energy and static stress drop of global subduction earthquakes from source time functions analysis, *Eos Trans. AGU* (Fall Meet.), **1,** 1 pp.

Cotton, F., R. Archuleta, and M. Causse (2013). What is sigma of the stress drop? *Seismol. Res. Lett.* **84,** 42–48, doi: 10.1785/0220120087.

Courboulex, F., A. Dujardin, M. Vallée, B. Delouis, C. Sira, A. Deschamps, L. Honoré, and F. Thouvenot (2013). High-frequency directivity effect for an M_w 4.1 earthquake, widely felt by the population in southeastern France, *Bull. Seismol. Soc. Am.* **103,** 3347–3353, doi: 10.1785/0120130073.

Dong, G., and A. S. Papageorgiou (2003). On a new class of kinematic models: Symmetrical and assymetrical circular elliptical cracks, *Phys. Earth. Planet. In.* **137,** 129–151.

Douglas, J., and H. Aochi (2008). A survey of techniques for predicting earthquake ground motions for engineering purposes, *Surv. Geophys.* **29,** 187–220.

Dreger, D. S., M. H. Huang, A. Rodgers, and K. Wooddell (2015). Kinematic finite-source model for the 24 August 2014 South Napa, California, earthquake from joint inversion of seismic, GPS, and InSAR Data, *Seismol. Res. Lett.* **86,** no. 2A, 327–334.

Dunham, E. M., and R. J. Archuleta (2004). Evidence for a supershear transient during the 2002 Denali fault earthquake, *Bull. Seismol. Soc. Am.* **94,** no. 6B, S256–S268, doi: 10.1785/0120040616.

Edwards, B., and D. Fäh (2013). A stochastic ground-motion model for Switzerland, *Bull. Seismol. Soc. Am.* **103,** no. 1, 78–98.

Godano, M., P. Bernard, and P. Dublanchet (2015). Bayesian inversion of seismic spectral ratio for source scaling. Application to a persistent multiplet in the western Corinth rift, *J. Geophys. Res.* **120,** no. 11, 7683–7712, doi: 10.1002/2015JB012217.

Hanks, T. C., and R. K. McGuire (1981). The character of high-frequency strong ground motion, *Bull. Seismol. Soc. Am.* **71,** no. 6, 2071–2095.

Heaton, T. H. (1990). Evidence for and implications of self-healing pulses of slip in earthquake rupture, *Phys. Earth Planet. In.* **64,** 1–20.

Houston, H. (2001). Influence of depth, focal mechanism, and tectonic setting on the shape and duration of earthquake source time functions, *J. Geophys. Res.* **106,** no. B6, 11,137–11,150.

Kanamori, H., and D. L. Anderson (1975). Theoretical basis of some empirical relations in seismology, *Bull. Seismol. Soc. Am.* **65,** 1073–1095.
Kanamori, H., and E. Boschi (1983). *Earthquakes: Observation, Theory, and Interpretation: Varenna on Lake Como, Villa Monastero*, Società italiana di fisica, North-Holland, 29 June 1982–9 July 1982.
Kanamori, H., and L. Rivera (2004). Static and dynamic scaling relations for earthquakes and their implications for rupture speed and stress drop, *Bull. Seismol. Soc. Am.* **94,** no. 1, 314–319.
Kaneko, Y., and P. M. Shearer (2014). Seismic source spectra and estimated stress drop derived from cohesive-zone models of circular subshear rupture, *Geophys. J. Int.* doi: 10.1093/gji/ggu030.
Kaneko, Y., and P. M. Shearer (2015). Variability of seismic source spectra, estimated stress drop and radiated energy, derived from cohesive-zone models of symmetrical and asymmetrical circular and elliptical ruptures, *J. Geophys. Res.* **120,** 1053–1079.
Kennett, B. L. N., and E. R. Engdahl (1991). Traveltimes for global earthquake location and phase identification, *Geophys. J. Int.* **105,** 429–465.
Madariaga, R. (1976). Dynamics of an expanding circular fault, *Bull. Seismol. Soc. Am.* **66,** 639–666.
Mai, P. M., and G. C. Beroza (2000). Source scaling properties from finite-fault-rupture models, *Bull. Seismol. Soc. Am.* **90,** 604–615.
Mai, P. M., and K. K. S. Thingbaijam (2014). SRCMOD: An online database of finite-fault rupture models, *Seismol. Res. Lett.* **85,** no. 6, 1348–1357.
Manighetti, I., M. Campillo, S. Bouley, and F. Cotton (2007). Earthquake scaling, fault segmentation, and structural maturity, *Earth Planet. Sci. Lett.* **253,** 429–438.
Margaris, B. N., and P. M. Hatzidimitriou (2002). Source spectral scaling and stress release estimates using strong-motion records in Greece, *Bull. Seismol. Soc. Am.* **92,** no. 3, 1040–1059.
Noda, H., N. Lapusta, and H. Kanamori (2013). Comparison of average stress drop measures for ruptures with heterogeneous stress change and implications for earthquake physics, *Geophys. J. Int.* **193,** 1691–1712, doi: 10.1093/gji/ggt074.
Shaw, B. (2013). Earthquake surface slip-length data is fit by constant stress drop and is useful for seismic hazard analysis, *Bull. Seismol. Soc. Am.* **103,** 876–893.
Thatcher, W., and T. C. Hanks (1973). Source parameters of southern California earthquakes, *J. Geophys. Res.* **78,** 8547–8576.
Tinti, E., L. Scognamiglio, A. Cirella, and M. Cocco (2014). Up-dip directivity in near-source during the 2009 L'Aquila main shock, *Geophys. J. Int.* **198,** no. 3, 1618–1631.
Vallée, M. (2007). Rupture properties of the giant Sumatra earthquake imaged by empirical Green's function analysis, *Bull. Seismol. Soc. Am.* **97,** no. 1A, S103–S114.
Vallée, M. (2013). Source time function properties indicate a strain drop independent of earthquake depth and magnitude, *Nat. Commun.* **4,** doi: 10.1038/ncomms3606.
Vallée, M., and E. M. Dunham (2012). Observation of far-field Mach waves generated by the 2001 Kokoxili supershear earthquake, *Geophys. Res. Lett.* **39,** no. 5, L05311, doi: 10.1029/2011GL050725.
Vallée, M., J. Charléty, A. M. Ferreira, B. Delouis, and J. Vergoz (2011). SCARDEC: A new technique for the rapid determination of seismic moment magnitude, focal mechanism and source time functions for large earthquakes using body-wave deconvolution, *Geophys. J. Int.* **184,** no. 1, 338–358.
Walker, K. T., and P. M. Shearer (2009). Illuminating the near-sonic rupture velocities of the intracontinental Kokoxili M_w 7.8 and Denali fault M_w 7.9 strike-slip earthquakes with global *P* wave back projection imaging, *J. Geophys. Res.* **114,** no. B02304, doi: 10.1029/2008JB005738.
Wells, D. L., and K. J. Coppersmith (1994). New empirical relationships among magnitude, rupture length, rupture width, rupture area, and surface displacement, *Bull. Seismol. Soc. Am.* **84,** 974–1002.

Françoise Courboulex
Université Nice Sophia Antipolis
CNRS, Géoazur, Observatoire de la Côte d'Azur
Valbonne, France
courboulex@geoazur.unice.fr

Martin Vallée
Agnès Chounet
Institut de Physique du Globe de Paris
Sorbonne Paris Cité
Université Paris Diderot
UMR 7154 CNRS
Paris, France
vallee@ipgp.fr
chounet@ipgp.fr

Matthieu Causse
ISTerre, IFSTTAR
University Grenoble Alpes, CNRS
F-38000 Grenoble, France
mathieu.causse@univ-grenoble-alpes.fr

Published Online 25 May 2016